Multiphase Fluid Flow via Multifilament Woven Fabrics: Lattice-Boltzmann Method

Dr. Mohammad Miyan

Department of Mathematics, Shia P. G. College, University of Lucknow, Lucknow, India.

Email: miyanmohd@rediffmail.com

ABSTRACT

The Lattice- Boltzmann method is used for the investigation of the dual scale problems of fluid flow through three dimensional multifilament woven fabrics. These fabrics are commonly characterized by two the different length scales i.e., the thickness of the single filament and the thickness of the bundle of filaments i.e., said as the yarn. The thickness of the yarn is of two orders of the magnitude greater than that of single filament. The inter-yarn and the intra-yarn spaces are of two different scales. The direct simulation of the fluid flow in the multifilament woven fabrics includes resolution of the flow in inter-yarn and intra-yarn pores of media.

In the present paper, there is an analysis about the fluid flow in the woven fabrics with the help of the Lattice-Boltzmann method. The tortuosities are also given by the LB simulations and the image analysis. The transverse and the in-plane tortuosities were analyzed by LB flow simulations and by the image analysis that uses chord length distribution algorithm [20]. The paper sheets formed as strictly layered structures in the laboratory sheet mold show little change in the tortuosity with the changing porosity as fibres were refined the density of the sheet was increased. Hence, transverse tortuosity has the significant change as the result of refining and densification. That indicates a less permeable and more complex structure. The chord length method tends to give higher values for tortuosity since the hydrodynamic tortuosity given by LB method gives more weight to the paths of the least resistance, whereas this method does not prefer any particular fluid path or chord length. The graphs show that the toruosity is inversely proportional to the porosity of media. The results are shown with the help of tables and figures.

Keywords: Flow, Lattice-Boltzmann method, Porous Media, Woven Fabrics.

I. INTRODUCTION

The woven fibrous porous media can be found in various industrial applications including but unlimited to preforming in the polymer liquid composite mouldings, filters for separation of the solid particles and the gas diffusion layer of proton exchange membrane fuel cells. The application that is of important use in the paper is the flow in the woven fabrics preform of the resin transfer moulding (RTM) process. The RTM process is an important method for manufacturing of both the small and large composite parts. The main problem in the RTM process is prediction of the resin flow in the mould through perform. So the knowledge of the resin flow pattern inside the mould is necessary for the determination of optimum location of the air vents and injection gates on the mould for reducing the possibility of the void formation in the manufactured parts. The preform is usually in the form of the multifilament yarns bound together in the different forms and structures. In this work, we focus on preforms constructed from woven fabrics;

Hu [10] and Chou [5] have discussed the properties and design of the micro structure of woven preform. Woven fabrics are characterized by two different length scales in general i.e., the length scale of a single filament, (e.g. its radius) and the length scale of a bundle of filaments i.e., yarns, which is usually about two orders of magnitude greater than that of the single filament.

Nabovati A. *et al.*, [14] have discussed deeply about the 3-dimensional multifilament of the woven fabrics. The woven fabrics have the dual porosity characteristics. The first defined porosity is related with internal structure of the yarn, and is known as the *yarn porosity* i.e., *y*. The yarn porosity gives the voids between the constituent filaments of the yarn and characterizes the intra-yarn flow. This is defined as the ratio of the void volume within the yarn to the total volume of the yarn. The second porosity is due to void spaces between the yarns and is known as the *weave porosity* i.e., *w*. Then for calculating weave porosity, the yarns are taken as solid *i.e*., zero yarn porosity; so the weave porosity is taken as ratio of void volume between yarns to the total volume of minimal bounding box of fabric sheet. The simulations of the fluid flow through woven porous media capture the flow through both yarn and weave porosities. The easiest structural form of the fibrous media that has been studied in analysis is the regular array of infinitely long solid cylinders. Gebart [6], Sangani [22] and Bruschke *et al.* [4] had studied the flow around solid cylinders of the infinite length with hexagonal and square arrangements and proposed correlations for transverse and axial flow permeabilities. The flow in solid yarn woven fabrics was first analyzed by using orifice analogy [4], [19], in this the pores between yarns were considered as the series of orifices and discharge coefficient was given as the function of pore structure.

Now, Lu *et al.* [12] analyzed numerically about fluid flow in monofilament filter cloth with the help of commercial software, employing finite volume method to simulate fluid flow in three bi-axial, basic, plain weave models for woven filters. By considering these three weave-models, four different pore structures were extracted to use in fluid flow simulations. The corrected form of the discharge coefficient in orifice model was based on the simulation results. Gooijer *et al.* [8] developed the geometrical model with orifice analogy, for flow resistance in monofilament woven fabrics with four unit pore structures of Lu *et al.* [12]. The proposed structure was in the good agreement with experimental data. By the methodology of Lu *et al.* [12], Wang *et al.* [23] simulated fluid flow in the unit cell of the monofilament woven fabric and given the values related to discharge coefficient for fabrics with the elliptical cross sections. From which, they were founded that the discharge coefficient decreases with increasing the aspect ratio of cross section of the fibres. By simulation of fluid flow in multifilament woven samples is challenging task due to dual scale nature of weave and yarn structures. But the direct simulation flow at both scales is computationally much expensive. So another popular approach is to simulate fluid flow for 2-dimensions in place of 3-dimensions. These simulations are of less demanding and they are not suitable to analyze the effects of curvature of yarns and their related structure on the overall permeability of multifilament woven fabric samples.

Papathanasiou [15] solved numerically the equation of Stokes in 2-dimensions with the help of the Boundary Element Method in square arrays of the permeable multifilament yarns, in that every yarn was made up of the circles representing the cross sections of constituent filaments. Now the effective permeability of medium was found as the function of weave and yarn porosities. In the similar patterns, the studies were performed for square and hexagonal arrangement of the filaments in the yarns, where the yarns had circular cross section [13] and for the yarns with the elliptical cross section [16]. Papathanasiou [17] had given the correlation for effective permeability of 2-dimensional hexagonal arrangements of filament clusters as a function of yarn and weave permeabilities given with the help of formula:

$$K_p = K_w \left\{ 1 + \alpha \left(\frac{K_w}{K_y} \right)^{n-\frac{3}{2}} \right\} \qquad (1)$$

Where K_p is effective permeability of multifilament fabric, K_w is weave permeability, K_y is permeability of cross-sections of yarns and α, n are constants related to geometric structure of fabric. The given relationship is based on the dimensional arguments and from consideration of behavior at the high and low *Kw/Ky* ratio asymptotes. Papathanasiou [17] had given values for n and α by fitting to numerical data and obtained the values as given:

(1.1) $\alpha = 2.3$ and $n = 0.59$; when filaments are arranged in the square array,

(1.2) $\alpha = 3.0$ and $n = 0.625$; when filaments are arranged in the hexagonal array.

It was claimed that the values of $\alpha = 2.67$ and $n = 0.61$ give a suitable fitting for both square and hexagonal ordered structures of the filaments in clusters and for high yarn and the low weave porosities. For the 2-dimensional case, the K_w and K_y depend on weave and yarn porosities, so that the arrangement of filaments inside yarns and arrangement of yarns themselves. The flow in the ordered structures of the cylinders has been studied deeply and various correlations for transverse permeability K, of the media have been given, in that the taken relationship is given by Gebart [6] is one of mostly used *i.e.,*

$$\frac{K}{R^2} = C\left\{\sqrt{\frac{1-\phi_C}{1-\phi}} - 1\right\}^{\frac{5}{2}} \qquad (2)$$

Where R is the radius of cylinder, ϕ is the porosity of medium, ϕ_c is the critical value of the porosity below which the fibres make contact and there is no permeating flow and C is the geometric factor depends on the type of packing;

Gebart's numerical analyses are as follows:

(1.3) $C=16/9\pi\sqrt{2}$, $\phi_c=1-\pi/4$ for square array of the cylinders,

(1.4) $C=16/9\pi\sqrt{6}$, $\phi_c=1-\pi/2$ for the hexagonal array.

The equation (2) will be used for predicting K_y by adjusting R equal to filament radius and ϕ equal to yarn porosity and K_w can be given by adjusting R equal to yarn radius and ϕ equal to weave porosity. The polymeric carrier fabrics are used in industrial processes mostly for the manufacturing of the paper and board. The 3-D structure of the fabrics gives a good role for deciding the manufacturing efficiency and energy of process and end used properties of product. Now the present analysis is based by using X-ray μCT to visualize the 3-D structure of polymeric fabrics commonly used in the paper manufacturing. The 3-D structural characteristics and fluid transport properties for tomographic images were measured with image analysis techniques and by the Lattice-Boltzmann method.

II. TOMOGRAPHIC IMAGES

The X-ray tomographic images were taken with the help of two different types of machine forming fabrics. The two samples of each type of wire were imaged. The resolution of the images was about 4.41 μm for the type I and 4.34 μm for the type II samples. A typical type of yarn with suitable diameter was with of order of 40 pixels, so the resolution of images was too good, as for the level of the discreteness effects. The lateral sizes of rectangular images were around one unit cell of wires that were about 2.3 × 2.2 mm^2 for type- I and 3.0 × 2.6 mm^2 for type-II wire. The samples images of type-I and type-II of wires are given in figures-1 and figure-2 respectively.

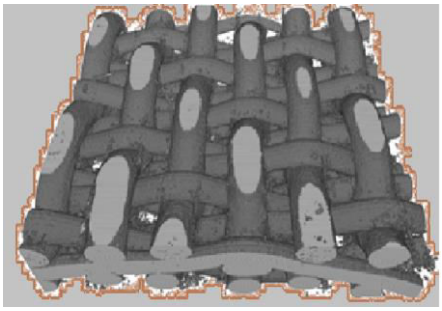

Figure-1 (Sample of the paper of type I)

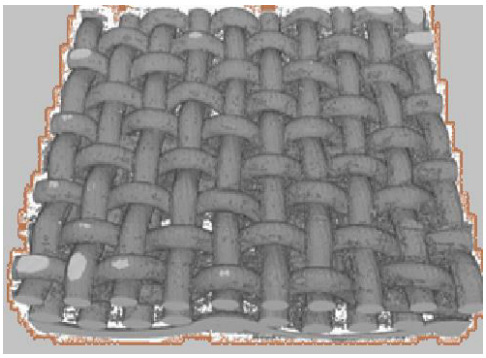

Figure-2 (Sample of the paper of type II)

The paper, wires can be utilized to some extent for analysis of quality of the used tomographic images, as we can expect to obtain the regular interior structure. Regarding this, we find from the images that the surface of wires seems spurious tiny and rough solid obstacles seem to be created by imaging process within the pore space. In the similar pattern, the solid phase seems to contain the incidental small voids.

So that the error created by the small irregularities can be observed to be very small *i.e.*, likely of small order. U. Aaltosalmi [1] analyzed in his researches by taking the three different sample papers *i.e.*, newsprint, filter paper and hand sheets were taken to observed the applicability of $X-\mu CT$ techniques. The hand sheet was made up of the bleached softwood Kraft pulp of spruce. The newsprint was made of thermo mechanical pulp of spruce in the paper machine and paper was not calendared. The filter paper was the circular black ribbon filter paper made of the cotton linters. The table: 1 shows the density, thickness and basis weight of imaged sample papers. The accuracies of these quantities are typically of order of the few per cent, so the samples taken have the distinct properties and characteristics, so that are expected to give some distinct results in image analysis and fluid transport simulations [1].

Table -1 (Bulk properties of imaged sample papers)

Sample papers	*Thickness (μm)*	*Density (kg/m^3)*	*Basis weight (g/m^2)*
Hand sheet paper	98	647	63.4
Newsprint	109	403	44.1
Filter paper	158	486	76.7

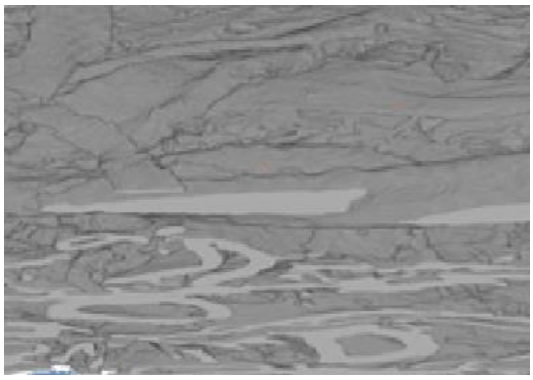

Figure-3(High resolution image of the paper)

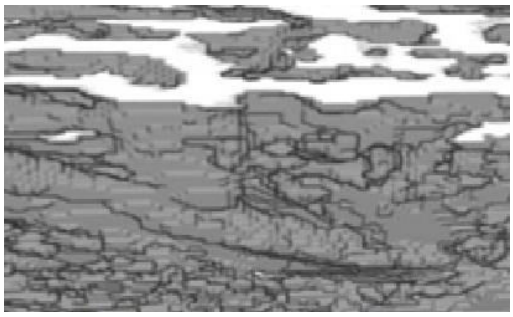

Figure-4 (Low resolution image of the paper)

Thus to identify the necessary level of the structural details for the reliable characterization of the different paper grades, U. Aaltosalmi used the samples imaged by using the low and high resolution $X-\mu CT$ techniques. The figure-3 and figure-4 show high and low resolution images of newsprint paper. The relatively small image sizes *i.e.*, less than 0.1 mm^2, were used in high resolution and various low resolution images. Also a set with the larger image size *i.e.*, about 1 mm^2, was taken for low resolution technique. The low resolution images were obtained by using the polychromatic radiation [11] and high resolution images were obtained by using the monochromatic synchrotron radiation in phase contrast mode [21]. The low and high resolution images were reconstructed and also processed according to routines [2], [11]. The small quantities of detached volumes of porous and fibrous phases were removed by 3-D filtering technique and surfaces of the samples were defined by using the rolling ball algorithm [3], [22]. Due to this, the surface is defined by route of the ball with a suitable radius that rolls towards the surface. The method allows the detection of main structures of the uneven surfaces excluding the interior pores [1].

The present image analysis techniques [11], [20] were used for determining the 3-D structural characteristics like specific surface area, porosity, hydraulic pore-radius distribution and diffusive tortuosity in principal directions. The diffusive tortuosity measurements were based on the various successful paths of the random walk simulation through paper volume with the random starting point on the suitable volume edge [1].

Table-2 (Some properties founded from the *3-D* images of the samples)

Sample papers	Image size	Resolutions	Thickness $T\ (\mu m)$	Density $\rho\ (kg/m^3)$	Basis weight	Porosity $\phi\ (\%)$	Specific surface area

					B_w (g/m^2)		$SSA(\times 10^3/m)$
Hand	Small	High	90.1	829	74.9	46.4	303
sheet	Small	Low	88.5	857	75.5	44.9	179
paper	Large	Low	101.5	796	79.6	49.0	176
News	Small	High	99.3	655	65.1	57.7	387
paper	Small	Low	119.2	651	76.1	58.2	179
	Large	Low	115.7	655	74.3	58.0	181
Filter	Small	High	190.9	550	105.5	64.3	234
paper	Small	Low	181.6	641	116.2	58.7	164
	Large	Low	179.4	570	101.8	63.4	157

The values were calculated in the principal directions by U. Aaltosalmi [1]. So, such flow related objects parameters as the tortuosity the flow paths and permeability of flow in transverse direction, were calculated by using the direct numerical simulations with the help of Lattice-Boltzmann method. There is use of specific *LBGK* model with the uniform external body force and bounce back boundary condition at the solid fluid interfaces. Then to ensure the unrestricted fluid flow at inlet and outlet, a free fluid layer with thickness of about 10% of the sample thickness was added on the top of sample and boundary conditions were imposed in all outer boundaries of rectangular computation volume. Now to compare the ability of techniques of imaging to find out correct amount of material in the imaged volumes, quantities of table: 1 *i.e.*, thickness, density and basis weight were calculated by the image analysis. The results shown by the table-2 are together with specific surface area and porosity.

Then in the followings, the values of the low resolution samples are the mean values obtained for the available samples. The slight differences between the image analysis and the bulk properties results obtained in part from normal variation *i.e.*, are related to formation of samples used but also from difference between the standard thickness, rolling ball defined thickness and from a probable over estimation of density of the fibres *i.e.*, used by the table-2 for all the papers. Hence used techniques may over estimate the volume of solid objects in images. The specific surface area for low resolution images is consistently less than that of high resolution images. Now the observed differences are mostly occurs due to differences in level of the details. So, it is clear from the visual comparisons that high resolution technique preserves topology of the porous structure and fibrous objects better than that of the low resolution technique. But the large volume images are much larger than that of the small volume images, and then there is no valuable difference between the characteristics and respective properties. That indicates that even small volumes are so suitable and sufficient for good estimation of the specific surface area and porosity.

III. TORTUOSITY AND PERMEABILITY

For the better analysis of the transport resistance of samples, their permeabilities and tortuosities were observed by U. Aaltosalmi, and the results are given by the table-3.

Table-3 (The tortuosity and permeability determined for various paper samples and imaging techniques)

Sample papers	Image size	Resolutions	τ_1	τ_2	τ_3	τ_4	ϕ
Hand	Small	High	2.69	3.47	16.0	3.78	0.0363
sheet	Small	Low	1.21	1.36	2.93	1.98	0.343
paper	Large	Low	1.25	1.36	3.25	2.11	0.325

News paper	Small	High	1.43	3.50	6.76	2.32	0.117
	Small	Low	1.12	1.56	3.57	2.04	0.524
	Large	Low	1.07	1.36	2.96	2.24	0.548
Filter paper	Small	High	1.23	1.33	4.69	1.58	1.95
	Small	Low	1.16	1.23	1.99	1.52	1.62
	Large	Low	1.10	1.17	1.61	1.55	2.78

In the table-3, τ_1, τ_2 and τ_3 are the diffusive tortuosity values in machine direction, cross direction and transverse directions respectively founded from the random walk simulations. The τ_4 and ϕ are the flow tortuosity and permeability in transverse direction obtained by direct numerical simulation and with the help of the Lattice-Boltzmann method.

The differences between the tortuosities, in different sample papers and also in the different principal directions, were observed in high resolution images, due to the higher level of detail. The smallest differences were found in small, low resolution images. The increase in resolution will increase the differences in measured tortuosity and will also improve the possibility of measuring the effects of paper structure on tortuosity and other characteristics and transport properties. The low resolution images will provide mainly right trends in these properties, so are useful for the comparative studies. Their applicability is limited by their lower ability to analyze the small particles such as fines, fibrils and fillers and fibre-orientation anisotropy. The flow tortuosity τ_4 was found to be systematically lower than that of the diffusive transverse tortuosity τ_3 .There are expectations since the streamlined hydrodynamic paths through the pore space are smoother than winding random walk paths of the diffusive particles.

So the dependence of flow tortuosity on the different structural properties of samples is similar to the diffusive tortuosity qualitatively and same qualitative analysis is better for both. About the results for flow tortuosity and permeability, there is no significant difference between the values calculated for large and small samples. Hence the permeabilities of low resolution images are higher than the high resolution images. The difference is then moderate at high porosities and will be significant at lower porosities. Then the poor resolution of low resolution images makes complex, dense structures more open for transport, whereas already open and relatively simple structures are affected lesser. Particularly, the high resolution results seem to be in qualitative agreement with known limiting behavior of the flow tortuosity. That would approach unity as porosity approaches unity and diverge at some small but non zero value of the porosity. In general, the results obtained for high resolution samples by Aaltosalmi U. [1] will be taken much reliable and better than others. The results discussed here, are qualitatively simple, they are with respect to uncertainty arising from limited available data and the calculations.

So to estimate the order of the magnitude of purely numerical errors rises from different used discretizations, there are the set of test samples by reducing resolution of original high resolution images to the low resolution images. The bigger difference between the permeabilities and tortuosities obtained for original high resolution samples and reduced resolution samples was about 20%. The error due to resolution could be compared to the sample size. The later was obtained by dividing original bigger images to others sub-images, the size of that coincided with that of the original smaller tomographic images. The greatest difference between the values calculated for original big image and mean value of corresponding sub-images was about 20% for tortuosity and 20% for permeability and these values are nearer to the values observed by using *Kozeny's* law. The conclusion is that the numerical uncertainties are not so suitable for qualitative results founded. Instead, the natural variation intrinsic to the paper material can be much more important source of the uncertainty for results obtained on tomographic images. Then the uncertainties in results are from the formation effect, to be of order of the second factor in tortuosity and permeability.

IV. Numerical Analysis

U. Aaltosalmi [1] analyses some numerical results of the fluid flow through tomographic images of the paper. The hand sheets of the basis weight of 300 g/m^2 were prepared from the bleached softwood Kraft pulp, which was beaten to the different refining levels between 220 and 670 *CSF* in a laboratory beater. The three dimensional $X-\mu CT$ images of samples were made by using phase contrast method [7], [9]. The resolution and size of images were about 2 μm and 1 mm^2 respectively. The paper surface layers were removed in direction of transverse axis, now the thicknesses of final samples lie between 120 μm and 200 μm. The examples of structures observed by tomographic imaging of paper samples are given by the figure-5. The images of these samples were observed for transverse and inplane permeability, specific surface area, porosity and tortuosity by using the image analysis techniques [7], [20] and Lattice-Boltzmann flow simulations in two orthogonal directions. So some reasonable comparison with the conventional mercury intrusion porosimetry data from the same samples was obtained [20].

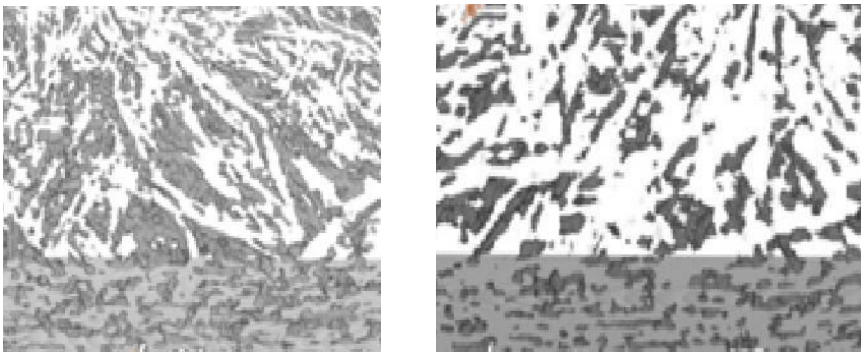

Figure-5 (The Tomographic images of the paper samples)

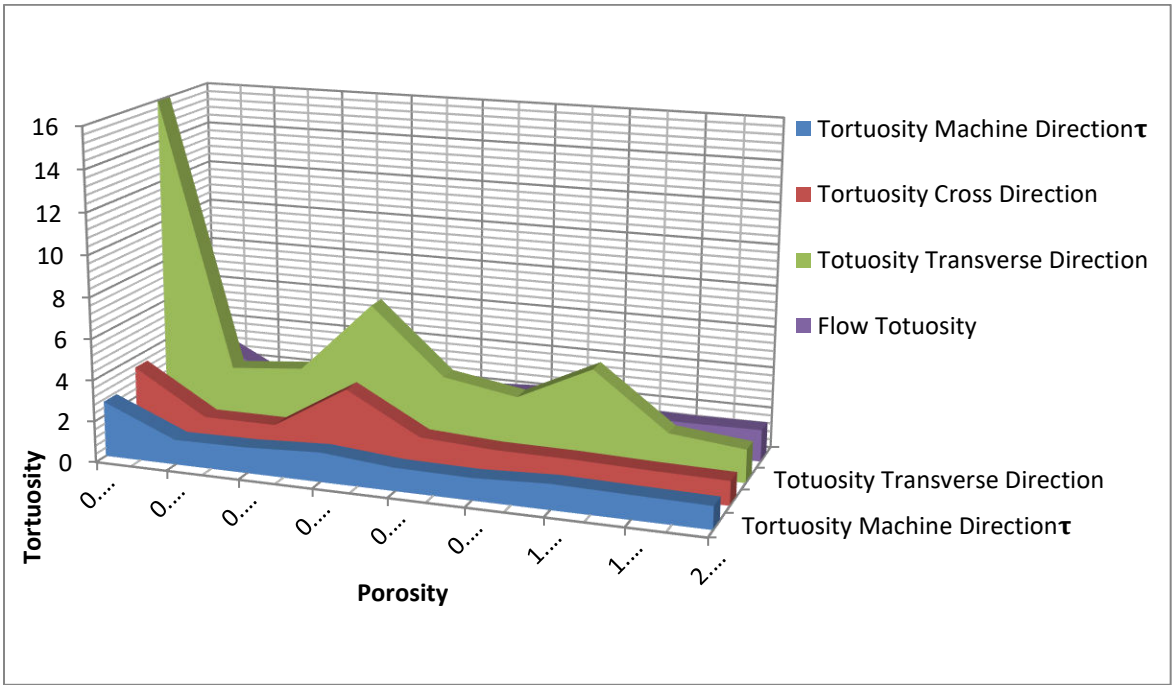

Figure-6

V. DISCUSSION AND RESULTS

The graphical representations with the data of table-3 are shown by figure-6. The figure-6 shows that toruosity varies inversely with porosity of media. The tortuosities are given by LB simulations and image analysis. The transverse and in plane tortuosities were determined by the LB flow simulations and by image analysis that uses chord length distribution algorithm [20]. The paper sheets formed as strictly layered structures in laboratory sheet mold show little change in the tortuosity with the changing porosity as fibres were refined density of sheet was increased. Hence, the transverse tortuosity has a significant change as the result of densification and refining. That shows a less permeable and more complex structure. The chord length method tends to give the higher values for tortuosity due to the hydrodynamic tortuosity given by LB method gives more weight to the paths of least resistance, whereas this method does not prefer any particular chord length or fluid path.

REFERENCES

[1] Aaltosalmi U. Fluid flow in porous media with the Lattice-Boltzmann method, University of Jyväskylä, *Research report No*. 3/2005, Finland, *pp*.39-45.

[2] Antoine C., Nygard P., Gregersen Q. W., Weitkamp T., Rau C. 3D images of paper obtained by phase-contrast X-ray microtomography: image quality and binarisation, *Nucl. Inst. Meth. Phys. Res*. A 490 (2002), *pp*. 392–410.

[3] Aronsson M. On 3-D fibre measurements of digitized paper, Ph.D. thesis, *Swedish University of Agricultural Sciences* (2002).

[4] Bruschke M.V., Advani SG. Flow of generalized Newtonian fluids across a periodic array of cylinders. *J Rheol* 1993; 37(3) *pp*. 479–98.

[5] Chou T. Microstructural design of fiber composites. Cambridge: *Cambridge University Press*; 1992.

[6] Gebart B.R. Permeability of unidirectional reinforcements for RTM. *J Compos Mater* 1992; 26(8) *pp*.1100–1133.

[7] Goel A., Tzanakakis M., Huang S., Ramaswamy S., Choi D., Ramarao B. V. Characterization of the three-dimensional structure of paper using X-ray microtomography, *TAPPI J.* 84 (5) (2001), *pp*.1-8.

[8] Gooijer H, Warmoeskerken M.M.C.G., Wassink J.G. Flow resistance of textile materials – Part I: monofilament fabrics. *Text Res J*. 2003;73(5), *pp.* 437–443.

[9] Gureyev T. E., Evans R., Stevenson A. W., Gao D., Wilkins S. W. X-ray phasecontrast microscopy of paper, *TAPPI J.* 84 (2), (2001), *pp*. 52.

[10] Hu J. Structure and mechanics of woven fabrics. Cambridge: *Woodhead Publishing*; 2004.

[11] Huang S., Goel A., Ramaswamy S., Ramarao B. V., Choi D. Transverse and inplane pore structure characterisation of paper, *Appita J.* 55 (3) (2002), *pp*. 230-234.

[12] Lu W.M., Tung K.L., Hwang K.J. Fluid flow through basic weaves of monofilament filter cloth, *Text Res J.* 1996; 66(5), *pp*. 311–23.

[13] Markicevic B., Papathanasiou T,D. On the apparent permeability of regular arrays of non uniform fibers. *Phys. Fluids* 2002; 14(9), *pp*. 3347–3349.

[14] Nabovati A., Llewellin E.W., Sousa A. C. M. Through-thickness permeability prediction of three-dimensional multifilament woven fabrics, Composites: Part A, 41 (2010), *pp*. 453-463.

[15] Papathanasiou T.D. On the effective permeability of square arrays of permeable fiber tows. *Int J Multiph. Flow* 1997; 23(1), *pp.* 81–92.

[16] Papathanasiou T.D., Gravel E.M., Barwick S.C. Non-isotropic structured fibrous media: the permeability of arrays of fiber bundles of elliptical cross section, *Polym. Compos.* 2002; 23(4), *pp*. 520–529.

[16] Papathanasiou T.D. Flow across structured fiber bundles: a dimensionless correlation, *Int J Multiph. Flow* 2001; 27(8), *pp*.1451–1461.

[17] Pedersen G.C. Fluid flow through monofilament fabrics, *In: 64th national meeting of AIChE*, New Orleans; 1969.

[18] Pedersen G.C. Fluid flow through mono filament fabrics, *Filtr Sep.* 1974; 11(6), *pp*. 586–589.

[19] Ramaswamy S., Huang S., Goel A., Cooper A., Choi D., Bandyobadhyay A., Ramarao B. V. The 3D structure of paper and its relationship to moisture transport in liquid and vapor forms, in: The Science of Papermaking - trans.*12th Fundamental Research Symposium*, Vol. 2, The Pulp and Paper Fundamental Research Society, Bury, Lancashire, UK, 2001, *pp*. 1281–1311.

[20] Samuelsen E. J., Gregersen Q. W., Houen P. J., Helle T., Raven C., Snigirev A. Three-dimensional imaging of paper by use of synchrotron X-ray microtomography, *J. Pulp Pap. Sci*. 27 (2) (2001), *pp*. 50–53.

[21] Sangani A.S., Acrivos A. Slow flow past periodic arrays of cylinders with application to heat transfer, *Int. J. Multiph. Flow,* 1982; 8(3), *pp*.193–206.

[22] Sternberg S. R. Biomedical image processing, *IEEE Comp.,* 16 (1), (1983), *pp*. 22–34.

[23] Wang Q., Maze B., Tafreshi H.V. On the pressure drop modeling of monofilament-woven fabrics, *Chem. Eng. Sci*. 2007; 62(17), *pp.* 4817–4821.